Electronic Supplementary Information (ESI)

Super compatible functional BN nanosheets/polymer films with excellent mechanical property and ultra-high thermal conductivity for thermal management

Jiemin Wang,[†a] Yuanpeng Wu,[†a,b] Ye Xue,[c] Dan Liu,[*a] Xuebin Wang,[d,e] Xiao Hu,[c] Yoshio Bando,[d,f] Weiwei Lei[*a]

[a] Institute for Frontier Materials, Deakin University, Waurn Ponds Campus, Locked Bag 20000, Victoria 3220, Australia.
[b] School of Materials Science and Engineering, Southwest Petroleum University, Chengdu 610500, PR China.
[c] Department of Physics and Astronomy and Department of Biomedical Engineering, Rowan University, 201 Mullica Hill Road, Glassboro, New Jersey 08028, United States.
[d] International Center for Materials Nanoarchitectonics (WPI-MANA), National Institute for Materials Science (NIMS), Namiki 1-1, Tsukuba, Ibaraki 305-0044, Japan.
[e] College of Engineering and Applied Sciences, Nanjing University, Nanjing 210093, China.
[f] Australian Institute for Innovative Materials University of Wollongong North Wollongong, NSW 2500, Australia.
† J. Wang and Y. Wu have contributed equally.

*Corresponding authors should be addressed at: dan.liu@deakin.edu.au (D. Liu) and weiwei.lei@deakin.edu.au (W.W. Lei).

1. Supplementary Methods:

The temperature distribution test of FBN/PVA films, Cu and Al foils:

In the experimental setup, an iron head was used as hot spot and insulated with a quartz tube to concentrate the heat. In addition, the top end of quartz tube was higher than iron head by 6 mm to protect the samples. Heat transfer experiments were conducted on copper foil, Al foil, and FBN/PVA film with same thicknesses (20 μm). Temperature of the iron dead was set to be 95 °C to avoid the oxidizing of the samples. All the samples were coated by graphite paint in order to get a same emissivity. The tested samples were put on a hot iron head, and an infrared thermal camera was used to record the temperature distribution under a steady-state.

The test of thermal conductivity (through-plane direction)

The thermal conductivity (through-plane direction) of the FBN/PVA films was analyzed by the device of ai-Phase Mobile 1u using a temperature-wave-analysis method according to ISO 22007-3. The samples were sandwiched between the heater and sensor plates. By scanning the frequency of heat source, the delay in the phase of the temperature wave was recorded within the range from -180° to -230 ° based on an empirical criterion. The linear fitting of phase lag θ *versus* square root of frequency, sqrt(f), was conducted to calculate thermal diffusivity a following

$$\theta = d \times \mathrm{sqrt}(\pi f / a)$$

where d is the thickness of samples. The thermal conductivity was further calculated based on the thermal diffusivity as well as theoretical density and specific heat capacity of composites.

The thermal conductivity was further calculated based on the thermal diffusivity as well as theoretical density and specific heat capacity of composites according to the rule of mixtures,

$$\rho_c = \phi_f \rho_f + (1-\phi_f)\rho_m,$$

$$c_c = \phi_f c_f + (1-\phi_f)c_m,$$

where ρ is the density, c is the specific heat capacity, ϕ is the volumetric filling fraction, and subscripts of c, f, and m indicate the composites, fillers and polymer matrices respectively.

The Calculation of Young's modulus of FBN/PVA films

For a classical composite material, the modulus change should follow the rule of mixtures:

$$E_c = \phi_f E_f + (1-\phi_f)E_m,$$

where E is Young's modulus, ϕ_f is the volumetric filling fraction, and subscripts of c, f, and m mean the composite, filler and polymer matrix, respectively. Yet the monotonic variation assumes that the filler, which usually has a much higher modulus than polymer, would become a crystal when ϕ_f becomes 1. However, the fillers are actually often powders, which have no strong bonding between particles, unless subjected to sintering Since pure FBN films are weak, as discussed above, the equation for the Young's modulus should be modified as

$$E_c = (1 - S_{Void}/S_f)\phi_f E_f + (1-\phi_f)E_m,$$

where S_{Void} represents the surface of BN untouched by polymers, and S_f is the total surface area of BN. If there is enough polymer, most of BN particles are surrounded by polymer molecules. When BN filling fraction is close to 1, a part of BN surface does not interact with polymer. Because there is actually little mechanical interaction between two BN filler sheets, these surfaces (S_{void}) actually do not contribute to the modulus, so S_{Void}/S_f will approach 1 when the filling fraction of BN approaches 1. The S_{Void}/S_f ratio is kept constant and is close to 0 for small filling fraction of BN. As a result, the modulus increases with increasing BN filling fraction at first. When the BN filling fraction approaches 1, the modulus does not reach that of single-crystal BN instead, it approaches the modulus of BN powder. When BN fraction increases heavily, the polymer matrix cannot provide enough "glue" to connect the flakes."

2. Supplementary Figures:

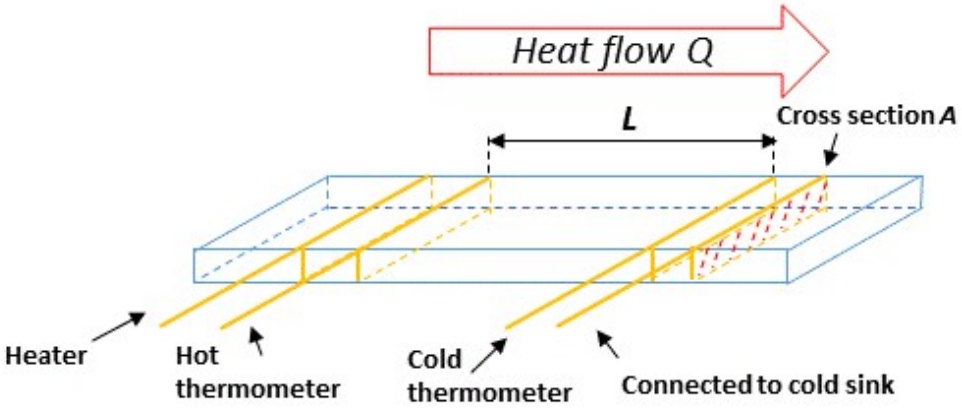

Fig. S1 Scheme for the thermal conductivity in-plane direction measurement setup.

The in-plane thermal conductivity of the FBN/polymer films was measured by a Physical Property Measurement System (PPMS, Quantum Design, USA) using the steady-state method. A film sample with a radiation shield is placed in a vacuum chamber (9.4×10^{-5} Torr) to minimize the radiation, convection, and conduction heat loss. The radiation heat loss is also calculated by the measurement system. Usually, the specimen is 4 mm × 18 mm with a rectangular shape. A heater shoe is connected to one end of the sample, and the other end is fixed to a cold sink. The hot thermometer shoe and cold thermometer shoe are both connected to the measured sample at a distance *L*. At steady state, the thermal conductivity (K) of the sample is determined by equation

$$K=(Q\times L)/(A\times \Delta T)$$

where *Q* is the net heat flowing through a known cross section *A* of the measured sample, ΔT is the temperature difference between the hot thermometer and cold thermometer, and *L* is the distance between the two thermometer shoes.

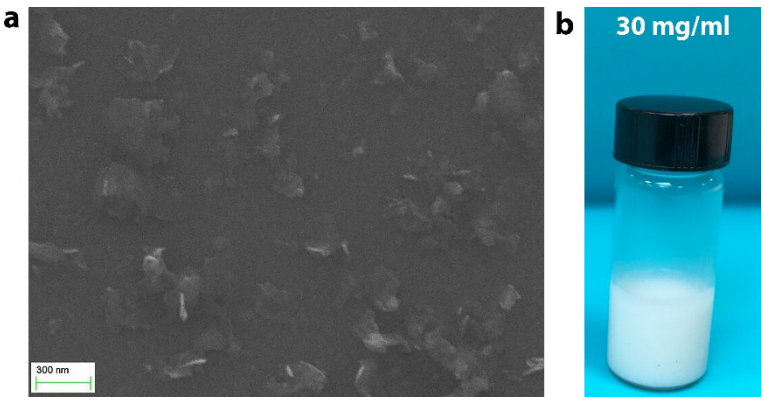

Fig. S2 (a) SEM images of FBN nanosheets and (b) the FBN water dispersion (30 mg/ml).

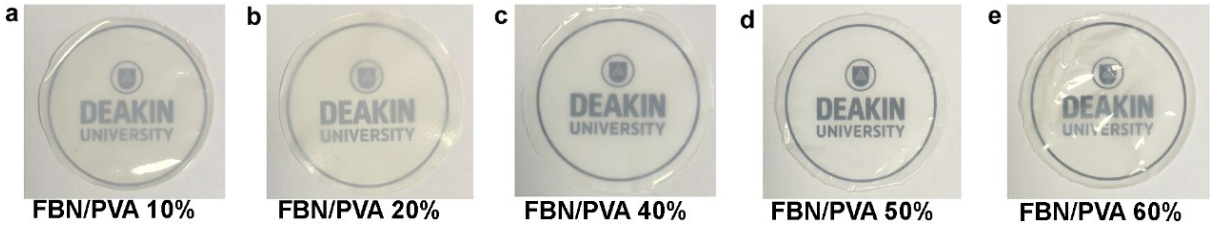

Fig. S3 Photos of FBN/PVA films. Photos of free-standing FBN/PVA10 wt%, 20 wt%, 40 wt%, 50 wt% and 60 wt% films placed over paper with a printed logo.

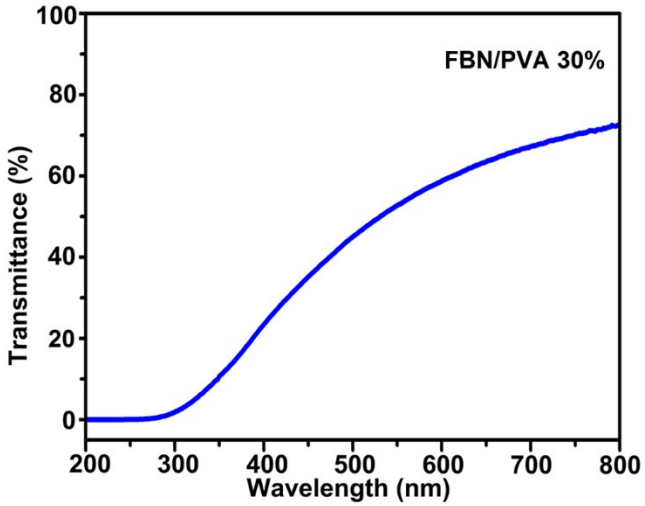

Fig. S4 Optical transmittance of the freestanding FBN/PVA 30 wt% films.

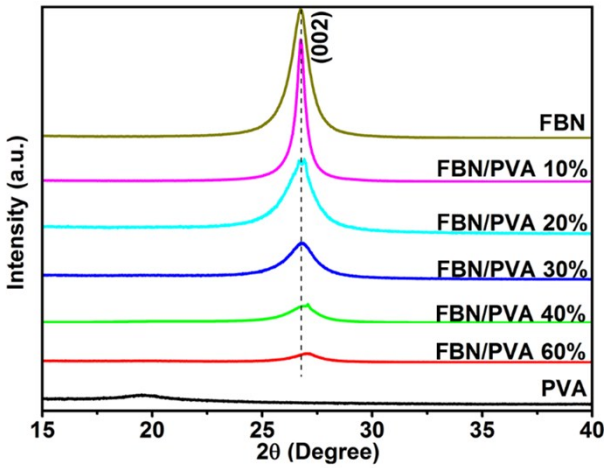

Fig. S5 XRD patterns of FBN/PVA films (PVA 10 wt%, 20 wt%, 30 wt%, 40 wt% and 60 wt%).

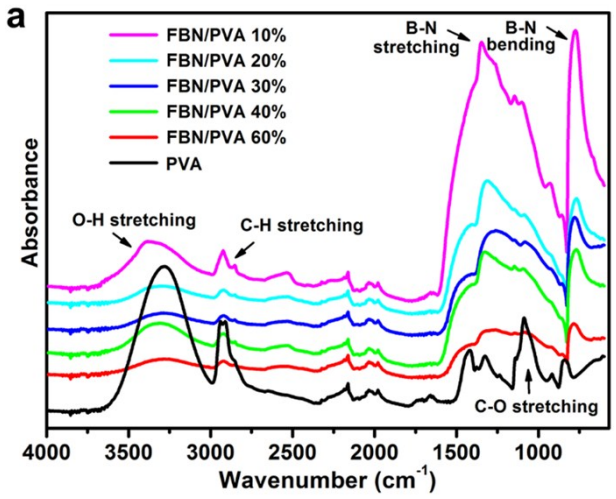

Fig. S6 FTIR spectrum of PVA and FBN/PVA films (PVA 10 wt%, 20 wt%, 30 wt%, 40 wt%, and 60 wt%).

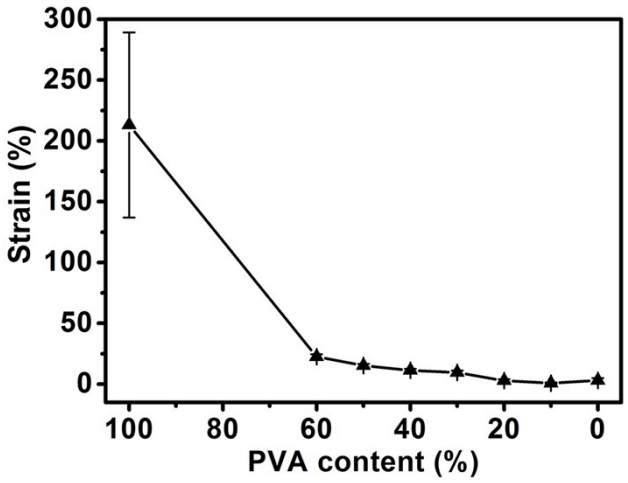

Fig. S7 The failure strain as a function of the PVA content.

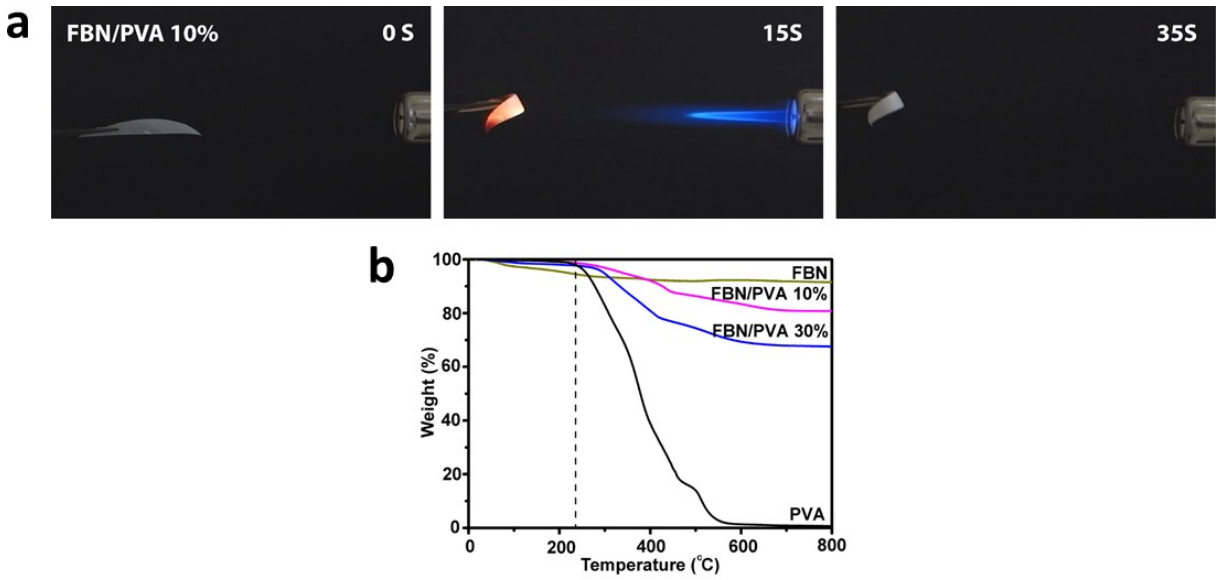

Fig. S8 (a) Fire-retardant properties of FBN/PVA 30 wt% and (b)TGA curves of FBN, PVA and FBN/PVA films.

Although the FBN/PVA 30 wt% is curved due to the surface tension when PVA section is under heating. However, it could be clearly observed that the composite membrane still remains un-ignited and keeps intact, demonstrating the fire resistance ability.

3. Supplementary Tables:

Table S1. The summary of mechanical properties of FBN/PVA films.

Samples	Young's modulus (MPa)	Tensile strength (MPa)	Strain to failure (%)
FBN	28.3 ± 10.6	7 ± 0.4	3.1 ± 1.8
FBN/PVA 10 wt%	1385.7 ± 129.1	21.2 ± 9.5	0.8 ± 0.6
FBN/PVA 20 wt%	989.2 ± 106.5	37.8 ± 7.9	2.9 ± 1.2
FBN/PVA 30 wt%	780.9 ± 95.4	78.3 ± 8.4	9.6 ± 1.5
FBN/PVA 40 wt%	809.3 ± 112.8	112.1 ± 8.7	11.4 ± 1.2
FBN/PVA 50 wt%	513.4 ± 76.3	103.8 ± 6.5	15.3 ± 1.4
FBN/PVA 60 wt%	458.2 ± 82.1	70.8 ± 8.1	22.5 ± 2.1
PVA	68.5 ± 31.3	47.9 ±10.3	213.1 ± 76.1

Table S2. Theoretical density and specific heat capacity of FBN/PVA films.

FBN/PVA films	Density g/cm^3	Thermal Capacity (J/Kg)
Pure FBN	2	0.79
FBN/PVA 10 wt%	1.87	0.871
FBN/PVA 20 wt%	1.76	0.952
FBN/PVA 30 wt%	1.66	1.033
FBN/PVA 40 wt%	1.57	1.114
FBN/PVA 50 wt%	1.5	1.195
FBN/PVA 60 wt%	1.42	1.276
PVA	1.2	1.6